

# NEW DEVELOPMENTS IN ATTITUDE CONTROL HARDWARE-IN-THE-LOOP TESTING

**Anja Nicolai<sup>(1)</sup>, Cloe-Marie Mora<sup>(1)</sup>, Roy Bretfeld<sup>(1)</sup>, Adrian Stroschke<sup>(1)</sup>, Vincent Delayat<sup>(1)</sup>, Heiko Jahn<sup>(1)</sup>, Christian Raschke<sup>(1)</sup>, Sebastian Scheiding<sup>(1)</sup>, Philippe Vidal<sup>(2)</sup>, Thomas Terzibaschian<sup>(3)</sup>**

<sup>(1)</sup> *Astro-und Feinwerktechnik Adlershof GmbH, Albert-Einstein-Str. 12, 12489 Berlin, a.nicolai@astrofein.com*

<sup>(2)</sup> *Airbus Defense and Space SAS, 31 rue des Cosmonautes, 31402 Toulouse Cedex 02, philippe.p.vidal@airbus.com*

<sup>(3)</sup> *Deutsches Zentrum für Luft-und Raumfahrt e.V.*

## ABSTRACT

Hardware-in-loop (HIL) testing of the Attitude Control System (ACS) is a proven concept for ensuring a reliable system in orbit. Combined with an air bearing, the performance of the ACS can be tested as close to in-orbit conditions as possible. For many years, the German Aerospace Center (DLR) in Berlin and Astro -und Feinwerktechnik Adlershof GmbH have been designing ACS and ACS components as well as performing ACS HIL tests. This led to the development of a state-of-the-art HIL ACS test bed, which has served ACS engineers throughout the world.

This paper shortly introduces the ACS test bed and describes the challenges of including the external reference system and the star simulation into the system. Also, the development of the NanoSat test bed is described and test results concerning the disturbance torques are presented.

Additionally, autocalibration of the CoG with a purely geometrical approach is described and test results are shown.

## 1 INTRODUCTION

A well-known and powerful tool for developing, testing and verifying an attitude control system (ACS) on the ground is a test bed with an spherical air bearing. It can almost perfectly simulate the low-torque situation of a satellite in space. The use of such an air bearing test bed is related to the test philosophy of a satellite project. It is the trade-off between purely analytical and software examination of attitude determination and attitude control algorithms or the use of hardware-in-the-loop simulation (HILS) and software-in-the-loop simulation (SILS) in conjunction with an air bearing test stand. Experience has shown that the tests on the air bearing test stands tend to reveal errors in the ACS algorithms that are not necessarily found with pure software verification, and have helped to avoid such surprises later in space.

The physical design of modern air bearing test stands is a combination of several components. There is the air bearing itself, the simulation of the satellite's moments of inertia (MOI) and the matching of the centre of gravity (CoG) with the air bearing's centre. The bearing itself and the deviations of the real centre of gravity from the ideal position introduce a residual disturbance torque, but at a level comparable to typical disturbance torques for small satellites in Low Earth Orbits (LEO).

The test bed can be extended to include geomagnetic field simulation for a given orbit and initial conditions, solar simulation, Global Navigation Satellite System (GNSS) simulation, and even star tracker simulation. An external reference system can also be included, that allows precise tracking of the movement of the device under test (DUT).

In the last decades, there has been a rapid development of such test beds for different classes of satellites from  $\mu$ -satellites (moments of inertia up to  $20 \text{ kg}\cdot\text{m}^2$ ) to nano-satellites and 1 U picosatellites.

## 2 THE ACS TEST BED

The heart of the testbed is the air bearing, which allows almost frictionless movement of the platform. The platform provides power to the DUT, so that no external cabling introduces disturbance torques. The platform also emulates the MOI of the DUT, so that only the components of the ACS and the on-board computer have to be placed on the platform. The platform also provides means for the calibration of the CoG, since placing it in the centre of rotation (CoR) is a crucial step for almost disturbance free testing. The platform also includes electronics for battery management, controlling the mass pieces for the wireless CoG calibration, communication with the test bed software and management of helpful tools like the inclinometer and the laser pointers. In its basic configuration, the test bed provides input for two attitude control sensors, the magnetometer and the sun sensors (and inherently, the gyros). A Helmholtz Coil system provides the opportunity to control any orbit-relevant magnetic field in any direction while simultaneously compensating the local magnetic field. The sun simulation provides input for the sun sensors, a versatile set-up consisting of a moveable lamp and mirror on an arc allows illumination from almost any direction.

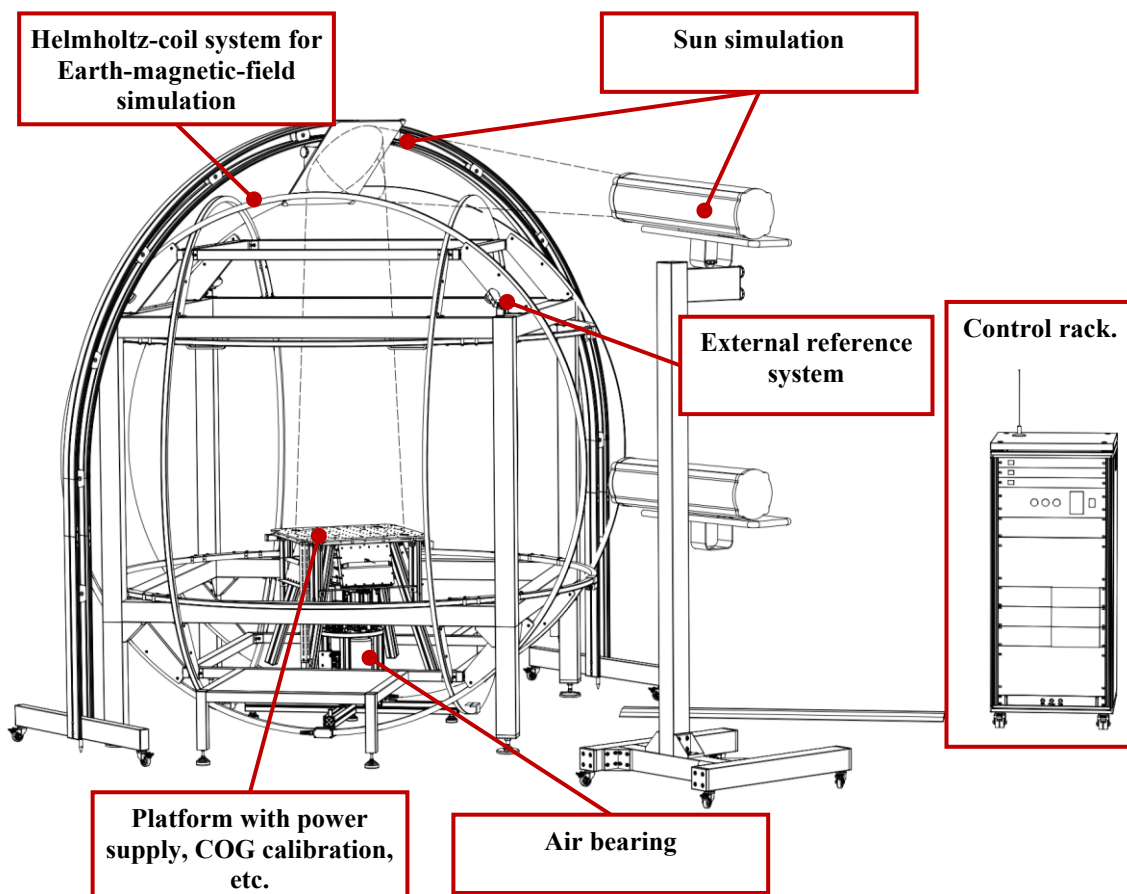


Figure 1 ACS Testbed

### 3 TEST ADVANTAGES AND TESTING EXPERIENCES

Initially, a first set-up with an air bearing to test attitude control algorithms was set-up at the DLR Berlin-Adlershof facility for the BIRD satellite, launched in 2001 [1]. The set-up consisted of an air bearing, Helmholtz coils and a sun simulator. Unfortunately, the connection to the DUT on the platform was realized with a wire, a constant source of disturbance torque, limiting the testing time. However, testing really did support the BIRD project and permitted to identify problems on ground instead of trouble shooting after launch [2].

The test bed set-up was much improved with the next satellite project TET-1 (launched 2012), a collaboration between the DLR Berlin and Astro- und Feinwerktechnik Adlershof GmbH.

Finally, the TET-1 engineering model (EM) was extended to also validate the ACS of the BIROS satellite (launched in 2016).



Figure 2 The equipped BIROS EM-ACS test stand in the clean room of Astro Feinwerktechnik Adlershof GmbH (2015)

Starting with rough qualitative checks of basic issues on the BIRD testbed (such as sensor/actuator signs, rate damping), testing on the TET-1 testbed extended to more use cases [2]:

- Sign verification (Sun sensor heads, gyro systems, magnetic field sensor, magnetic torque rods, reaction wheels)
- Attitude determination algorithms from simple Sun vector, B-vector estimation, over quaternion estimations, Sun rate, B-rate, quaternion-rate estimations, model-based attitude estimations from observed Sun and B-vectors
- Fault-Detection, Fault-Isolation and Recovery (FDIR) algorithms, FDIR on ground support for the flying satellite
- Attitude manoeuvre tests (rate damping, slews, pointing including bias rates and angles (e.g. Sun pointing, inertial pointing, target pointing on Earth, nadir pointing for up > 90 min test time / one orbit)
- Full tests of all ACS specific telemetry (TM) and telecommands (TC) including TC parameters, verification of the mission information base (MIB)

- Test of flight procedures for mission control and operations
- SW verification tests before every SW upload to the satellite flight model (before and after launch)

The experiences with these air bearing test stands led to a new product line at the company with extensions of the available dimensions in mass, inertia, power, accuracy and other technical features due to customer requirements.



Figure 3 State-of-the-art facility for a customer at Astro Feinwerktechnik Adlershof GmbH

## 4 TESTBED COMPONENTS AND EXTENSIONS

The state-of-the-art testbed consists of the basic system described in section 2, and optional extensions depending on ACS simulation needs.

### 4.1 Air bearing and Platform

The air bearing provides a low disturbance, almost frictionless movement of the platform attached to it. Disturbance torques are in the range of  $<10^{-5}$  Nm around the z-axis (vertical axis) and  $\sim 2 \cdot 10^{-4}$  Nm around the x/y-axis. They are comparable to the disturbances seen by the small satellite class in LEO and therefore allow validation of highly agile ACS modes and / or long time tests.

The platform attached to the air bearing fulfils multiple functionalities. It is the interface to the DUT, providing a mounting surface as well as a regulated power supply with different voltage levels. ACS components can be mounted on the table and connect directly to the platform's power supply. The platform also emulates the MOI of the whole satellite. Additional masses and different platform configurations (see Figure 4) allow MOI setting between 3 – 20 kgm<sup>2</sup>. The platform also provides the means to calibrate the CoG. Small 100 g masses can be precisely and wirelessly moved in each axis to fine tune the CoG position. The calibration process can be tedious and requires experience. On the one hand, training in the facility focuses on that point and on the other hand,

new developments are looking into an autocalibration technique (see section 4.3).

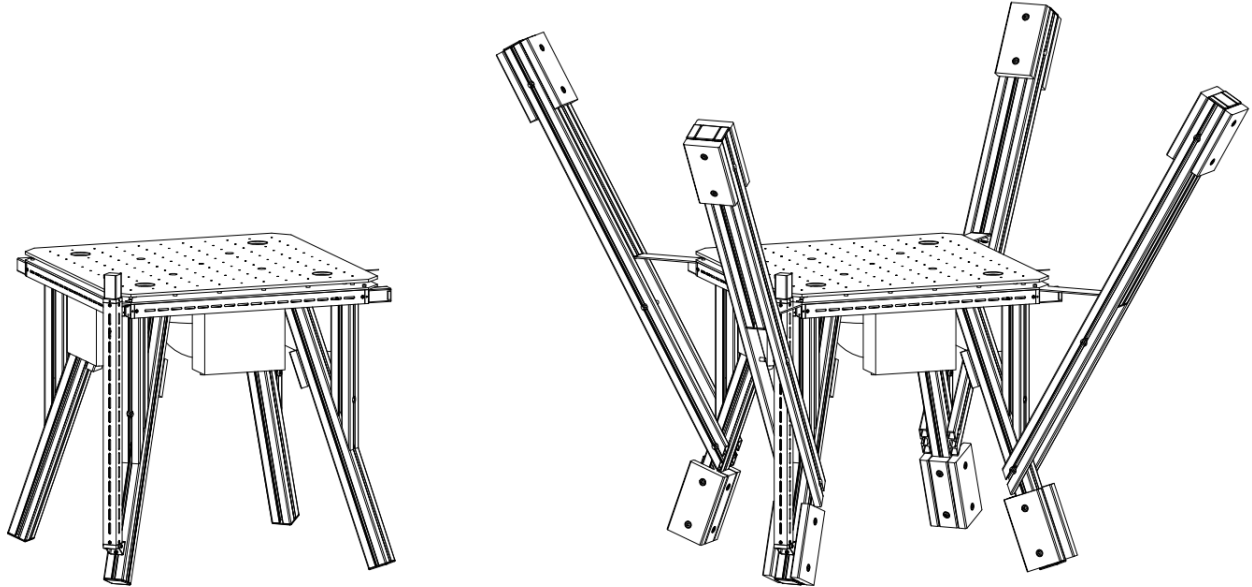


Figure 4 Platform configuration for min. MOI (left) and max. MOI (right)

## 4.2 External Reference System

It is incredibly useful during ACS testing to have an external reference system indicate the actual position of the platform. This helps verify the performance of the ACS. The commercial optical tracking system Optitrack was chosen [3], a well-proven system for motion capturing. Markers made from a reflective material are placed on the tracked device (in our case: the platform). At least four cameras are placed on the top of the Helmholtz cage frame. They emit infrared light, which is reflected by the markers and detected by the cameras. In the “Motive” software, this information from every camera is combined to precisely detect the position of each marker. Different markers can be combined to define a “rigid body” whose movement is then tracked. Position and rotation information can then be recorded and / or streamed, for example in the form of quaternions.

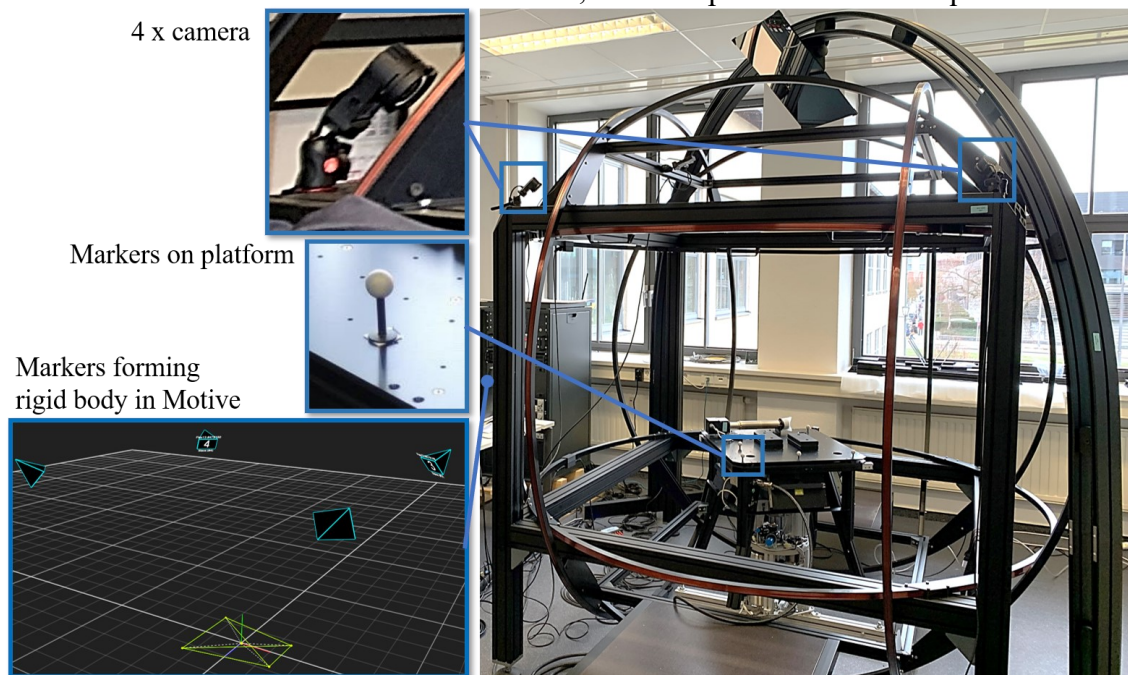


Figure 5 Optitrack System installed on Testbed and corresponding set-up in Motive

### 4.3 Autocalibration

Manual calibration of air-bearing systems is a common method to reduce disturbance torques. The coincidence point of the CoG and the CoR can be found where it is observed that the platform neither topples nor swings as a pendulum. The system, however, is highly sensitive to touch, air currents, air friction, and other physical variables. Where one might observe the CoG to be coincident with the CoR, a disturbance in the air can reveal the CoG to be too high or too low by a factor as small as half a millimetre. Additionally, the process of calibration can be tedious, taking a long time especially for large MOI configurations and requiring experience and training.

To improve on this, varied methods of autocalibration have been developed. These methods generally rely on estimation of the entire system's moment of inertia matrix using CAD models [4] or batch estimation methods [5]. However, this requires generating a new matrix estimation with each new test subject that is mounted to the platform, which is not ideal for a test bed that frequently tests different ACS components or satellites at a time. Therefore, an autocalibration procedure has been developed that is bound only by the known physical parameters of the system and does not require inertia estimations.

When the CoG of the system rests below the CoR of the air bearing, the platform will behave as a pendulum oscillating about the CoR. The pendulum behaviour of the platform in this configuration introduces corresponding dynamics that can be exploited to find the offset of the CG from the CR.

A force analysis of the platform as a pendulum yields the equation for a harmonic oscillator,

$$\ddot{\theta} + \omega^2 \sin\theta = 0 \quad (1)$$

where the natural frequency is given by  $\omega = \sqrt{\frac{g}{l}}$ . In the context of this system as a pendulum,  $l$  is the distance of the CoG from the CoR, and  $\theta$  is the angle of the pendulum (which is equal to the angle between the platform and the horizontal plane) during oscillation. The vector  $l$  is given by  $l^2 = l_x^2 + l_y^2 + l_z^2$ , and can be visualized in Figure 6, with the CoR at the centre of the coordinate frame and the vector  $l$  stemming from the CoR to the CoG. A torque analysis then defines the angular acceleration as

$$\ddot{\theta} = \frac{-mgl \sin\theta}{I} \quad (2)$$

where  $I$  is the moment of inertia of the system and  $m$  is the system mass. Implementing this definition in the equation for a harmonic oscillator (1), as well as the definition of angular frequency  $\omega = \frac{2\pi}{T}$ , the period of the platform oscillation can be solved for as

$$T = 2\pi \sqrt{\frac{I}{mgl}} \quad (3)$$

The moment of inertia is unknown, but the necessity for its estimation can be eliminated by capitalizing on known values.

The autocalibration process begins by roughly calibrating the horizontal axes, and then intentionally lowering the CoG several centimetres below the CoR. In this way the offset in the vertical axis is significantly larger than the offsets in the horizontal axes ( $l_x$  and  $l_y$ ), which become negligible such that  $l_z$  can be considered the  $l$  of the system. While  $l_z$  is unknown, the moveable masses allow the user to change the position of the CoG by a value  $dl_z$ . By inducing a pendulum and measuring the period of the system, then moving the CoG a known distance and measuring the period again, the change in period  $dT$  and the change in CoG position  $dl_z$  can be used to solve for the unknown offset  $l_z$ . The period of the platform oscillations is measured using data gathered by the optitrack system (section 4.2).

Moving the vertical mass  $m_z$  downwards a known distance  $dz$ , the corresponding change of position of the CoG can be found using

$$dl_z = \frac{m_z dz}{m} \quad (4)$$

This change in position is also naturally given by

$$dl_z = l_{z1} - l_{z2} \quad (5)$$

Referencing the period equation (3), the mass  $m$ , gravity  $g$ , and moment of inertia  $I$  remain constant for each data set. Using this, the period equation can be manipulated and the initial and second calculations for the periods can be set equal to one another such that  $T_1^2 l_{z1} = T_2^2 l_{z2}$ . From here,  $l_{z2}$  can be replaced using equation (5) and  $l_{z1}$  can be solved for such that  $l_{z1} = \frac{-T_2^2 dl_z}{T_1^2 - T_2^2}$ . This gives the initial distance of the CoG from the CoR. Now equation (5) can be used to calculate  $l_{z2}$ , that is to say, the remaining distance of the CoG from the CoR. The operator can only manipulate the moveable mass, so the calculated value of  $l_{z2}$  then serves to calculate the distance needed to move the vertical moveable mass

$$dz_{new} = \frac{l_{z2} m}{m_z} \quad (6)$$

in order to close the offset between the CoG and the CoR.

With the vertical offset accounted for, similar logic is applied to the horizontal axes. When the platform's horizontal axes are calibrated, and pendulum motion is induced, the horizontal axes will rotate around zero. When there exists displacement of the CoG in either horizontal axis, the respective axis will rotate around the resulting displacement. The angle of rotation of each axis can be plot from the sensor data (section 4.2), and from there the angle of displacement can be found. These displacement angles can be physically defined as

$$\tan(\theta_x) = \frac{l_y}{l_z} \quad (7)$$

and

$$\tan(\theta_y) = \frac{l_x}{l_z} \quad (8)$$

Using the known value of  $l_z$  from the vertical calculation process, the offsets  $l_x$  and  $l_y$  can be calculated (Figure 6).

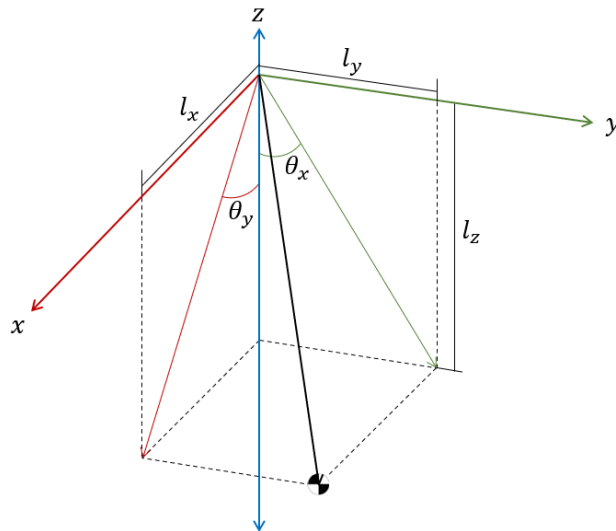


Figure 6 Projection of vector  $l$ , and the resulting geometries, with the CoR at the origin.

To test this method, the platform is first manually calibrated, and the corresponding position of the balance masses recorded. From here, the vertical mass was lowered a known distance. This value is later used to determine the validity of the calibration, by acting as an expected value for the results

of the calibration. Once lowered, the oscillation of the platform is induced. It was shown after several trials that best practice is to induce the pendulum motion from a corner of the platform, to ensure that a significant period is triggered along both the x- and y-axis, to improve the period calculation. This initial period is calculated, and then the vertical mass is shifted upwards ( $dz$ ). Oscillations are once again induced, the new period is calculated, and finally the distance needed to close the CoG-CoR offset is calculated.

Similarly, the horizontal calibration can also be done after the vertical mass has been lowered initially. Intentional offsets were also made using the x and y masses, which were then used as a reference for the calibration output, and then oscillations were induced. The angles of rotation along each axis were determined, and with that their respective offsets.

Comparing the results of the calibrations, that is to say, comparing the recommended distances needed to move the balance masses with the intentional offsets given, showed the success of the calibration. Figure 7 shows the difference between the expected value (the intentional offset) and the calculated values from the calibrations. The dotted line at 0.5 cm on the vertical axis plot (right) is to give reference to the gap that is generally left from manual calibration. It is difficult to determine the vertical offset manually; general practice is to calibrate the CoG slightly below the visually estimated CoR (a distance equivalent to moving the vertical mass by approximately 0.5 cm which is roughly 6  $\mu\text{m}$  distance between CoG and CoR). This is done to ensure that any external variables from the environment do not cause the platform to tip. Acknowledging this, the test results can be compared based on their difference from this baseline, rather than zero, as manual calibration is not so accurate. As can be seen in Figure 7, the majority of the calibration results are calculated within one centimetre of the expected results. When these values were implemented, the platform was found to be visually stable. The recommended autocalibration process in its entirety can be completed within an hour and can be implemented by any operator with limited to no prior training. Attempting accurate manual calibration with an experienced operator in a small MOI configuration can take up to an hour, but with an inexperienced operator or with a large MOI configuration it becomes a process that takes several hours or even up to two days. Implementation of this autocalibration will significantly improve the time needed to calibrate the system and will greatly reduce human error that is inherent in manual balancing.

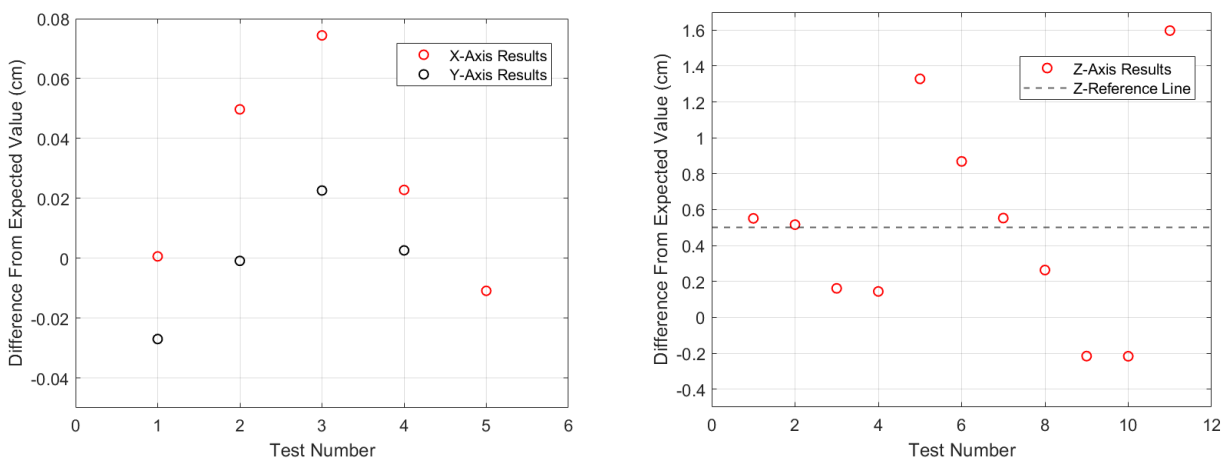


Figure 7 Results of calibrations in reference to expected values (horizontal axes left, vertical axis right).

#### 4.4 Magnetic Field Simulation

The magnetic field simulation consists of a Helmholtz cage with a maximum diameter of 2.4 m and three high-precision bi-polar power supplies. By calibrating each coil, a 1% magnitude precision is reached in the centre and <3% deviation in magnitude in a  $\text{Ø}50$  cm sphere around the centre. The maximum achievable field in this set-up is 200  $\mu\text{T}$  per axis, but stronger field set-up can be done.

The testbed control software includes the interface to the power supplies and a manual magnetic field can be commanded in any direction or a field according to the current orbit position from a Simplified General Perturbation Model (SGP4) propagator using the current International Geomagnetic Reference Field (IGRF) model. Also, the orthogonality of the field in the centre is measured and a correction matrix can be set in the software, thus reducing the orthogonality error to  $<1^\circ$ .

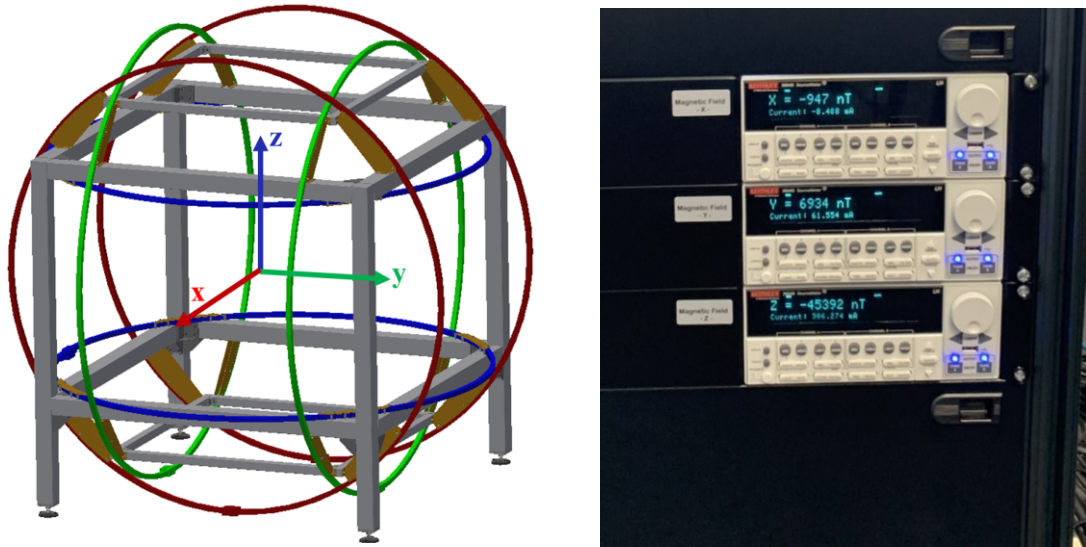


Figure 8 Helmholtz cage for magnetic field simulation (left) and power supplies integrated into the control rack

#### 4.5 Sun Simulation

The sun simulation is a 600 W LED lamp providing Illuminance in the range of sun light (50 000 – 120 000 lux) The illumination circle in 3 m distance is 500 mm with a collimation of the light beam of  $7.5^\circ$ . A flexible set-up with moveable sun and mirror assembly (see Figure 9) allows the sun in any direction. The ACS Control Software calculates the sun vector for each simulated scenario and also indicates umbra times.

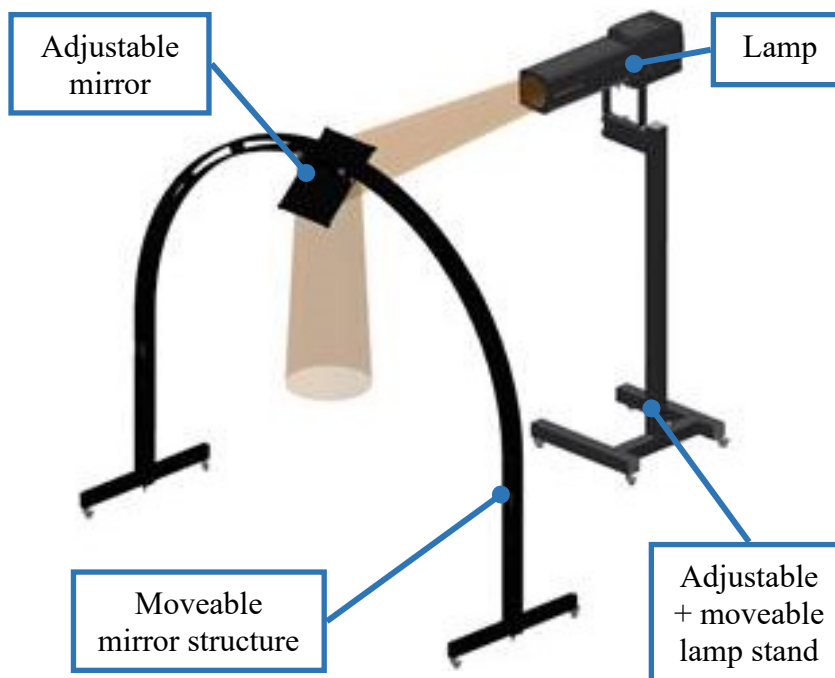


Figure 9 Lamp and mirror assembly to complete sun simulation

## 4.6 GNSS Simulation

For some satellites, accurate position information in orbit is crucial for mission success and thus needs to be included in HIL tests. There are common GNSS simulation systems available and in the past, Spirent systems have been included in the testbed by synchronizing the test bed software ACS control with the Spirent simulation software using the remote control function.

## 4.7 Star Simulation System

Most satellites ACS contain a Star Tracker to precisely determine the satellite's attitude in an inertial reference frame. Adding a star simulation capability to the test, is therefore a logical step. Airbus has been building Star Tracker Optical Stimulators (STOS) since 1998.

As input, the STOSPilot software application which is running on the STOS calculator receives (or locally compute) current star tracker attitude in an inertial reference frame. Using this information, the application scans a star catalogue and determines which star is visible and must be displayed in the field of view. In addition to the starry sky image, the following disturbances can be added: these can be additional stars that are not in the current catalogue, planets, extended objects, additional moving stars (to simulate debris or satellite crossing the field of view), background and stray-light, protons effect and a specific moon model that simulates blooming on detector pixels.

Image calculation by the STOS calculator lasts less than one millisecond. Once calculated, the image is updated in the graphic memory and then sent to the opto-mechanical assembly (OMA) which displays the corresponding image and send it to the star tracker optics using a collimator. The star tracker can then determine attitude depending on the projected stars as if looking at the real sky.

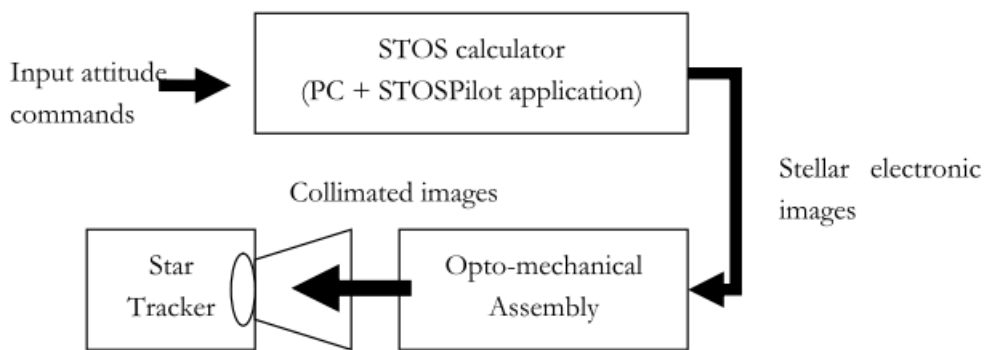


Figure 10 Schematics of the Star Simulation System

The focal plane of the stimulator is based on a Ferroelectric Liquid Crystal on Silicon (FLCOS) reflective micro display element and uses the principles of Time Domain Imaging (TDI) to build the images: the principle is that each pixel acts like a micro mirror array by reflecting or not input light generated by the illumination system. Thus, the required brightness (depending on pixel value) is obtained by temporal modulation of the ON-OFF state of the pixel. The micro display element is located in the focal plane of a collimating tube equipped with an objective (on display side) and an eyepiece (on star tracker side).

Thanks to dedicated electronics integrated inside the OMA, the HDMI signal coming from the PC graphic board is processed into adequate signals before being sent to the display.

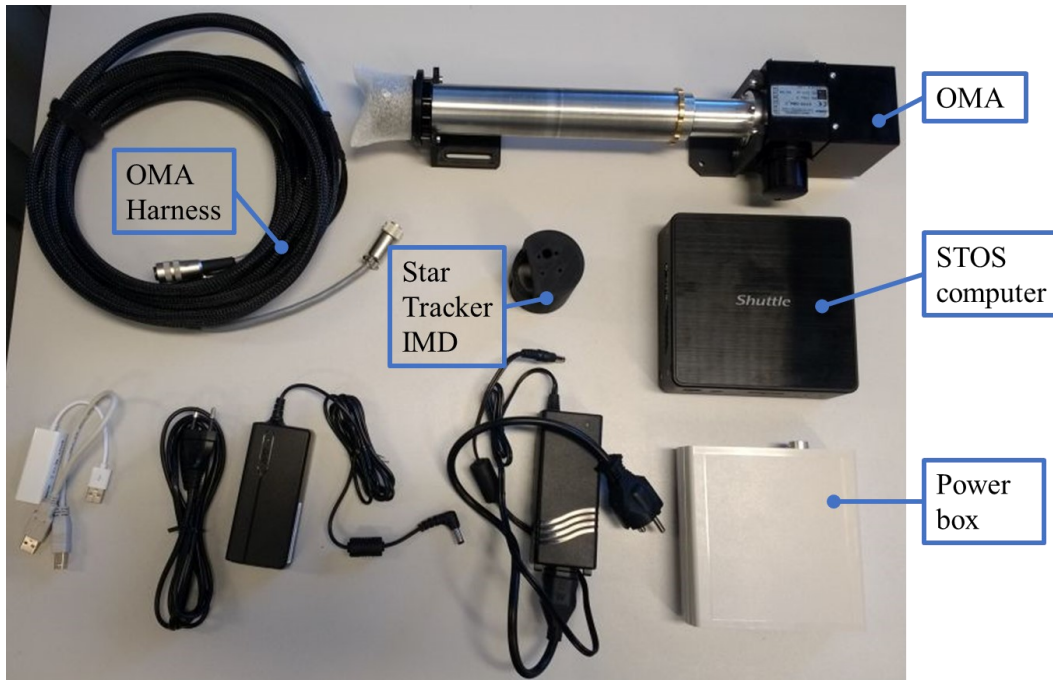


Figure 11 STOS components, not showing monitor, keyboard and computer mouse

The ACS testbed incorporates the Star Simulation System, which integrates several components: Motive optitrack (refer to section 4.2), the orbit propagator (refer to sections 4.4 and 4.5), and the STOS. The platform attitude is acquired by the ACS Control software (via the Motive software), which applies filtering and transformations based on user-defined parameters. The filtered data, along with the Nadir, Sun and Moon vectors, is then transmitted to STOS. STOS buffers, interpolates, and renders the data, simulating the spacecraft attitude using a selected Star Tracker and star catalogue. Finally, the rendered image of the stars is output via HDMI and then wirelessly transmitted to the Opto-Mechanical Assembly (OMA) mounted on the platform.

The general data management and display is done within the ACS-Control software in a specific module referred to as the StarTracker-Manager (ST-Manager) using the Application Programming Interfaces (API) from Motive and STOS.

By integrating their entire Attitude Control System directly onto the platform, engineers can test even more scenarios and sub-systems at once and achieve a closer approximation to real in-orbit situations. However, this integration poses certain challenges, particularly in terms of positioning precision and the occurrence of delays during data transfer and management.

The Motive optitrack system measures the platform attitude with a maximum resolution of 0.1mm per InfraRed tracker. This allows for an accuracy in the star reference system down to approximately  $0.01^\circ$  depending on the calibration accuracy and the exact platform attitude. Preliminary tests show a spread of up to  $0.41^\circ$  deviation. Some jitter and noise also need to be compensated which is done in two different ways, the first one being a sliding average within the ST-Manager, and the second one by buffering and interpolating the data within the STOS software (in order to reduce jitter).

To achieve this accuracy, limit the jitter and enable a necessarily wireless connection between the platform and the computers, some delays are unavoidable and need to be taken into consideration. Depending on the Motive acquisition (up to 120 frames per second, 5 to 10ms delay), the buffer size for the sliding average (nominally 60 points, where a bigger buffer means less noise but also eventually degrades the actual data) and the buffer size and transfer speed to the STOS software (nominally 200ms, where a bigger buffer improves system stability, but increases the delay), the delay measured in a recommended configuration can go up to 500 to 600ms with the wireless HDMI connection (estimated below 10 ms).

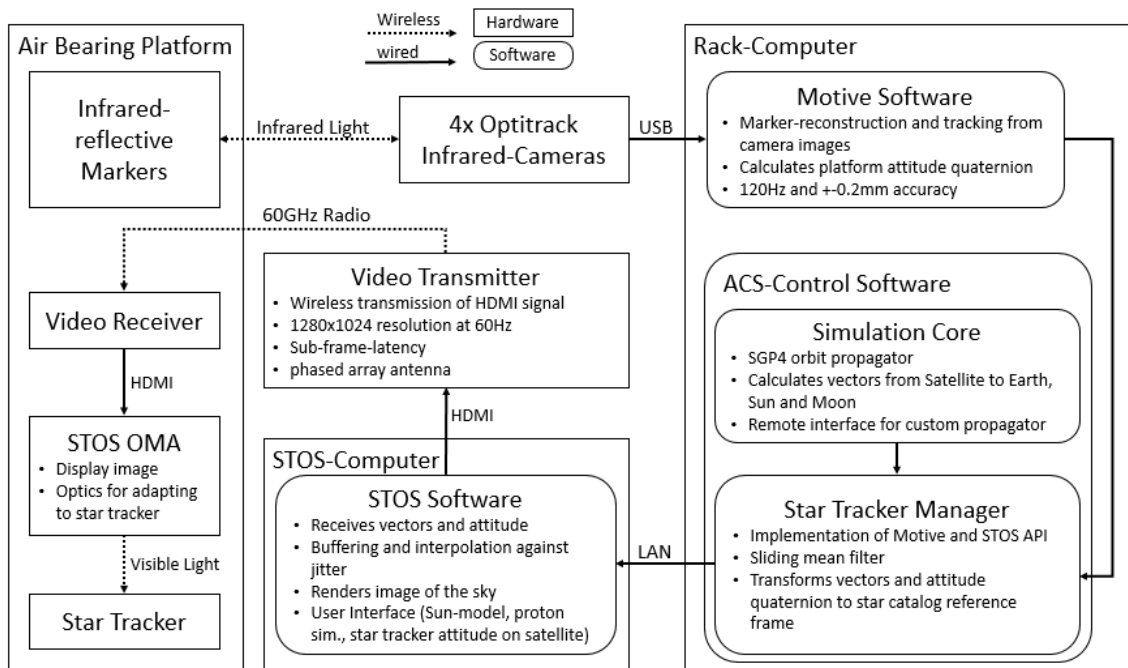


Figure 12 Interface description of the Star Simulation System

Whether or not this level of accuracy and delay are acceptable will depend on the test case and the Star Tracker selected: for a high rotational speed test, the noise and accuracy will be less relevant than the delays and jitter induced, while for a slow rotational test, the delays induced will be less important compared to high accuracy required with low noise.

The ST-Manager allows the user to change various settings to accommodate for specific test settings, including changing the reference frame and the transformations to apply in order to match the star catalogue reference system.

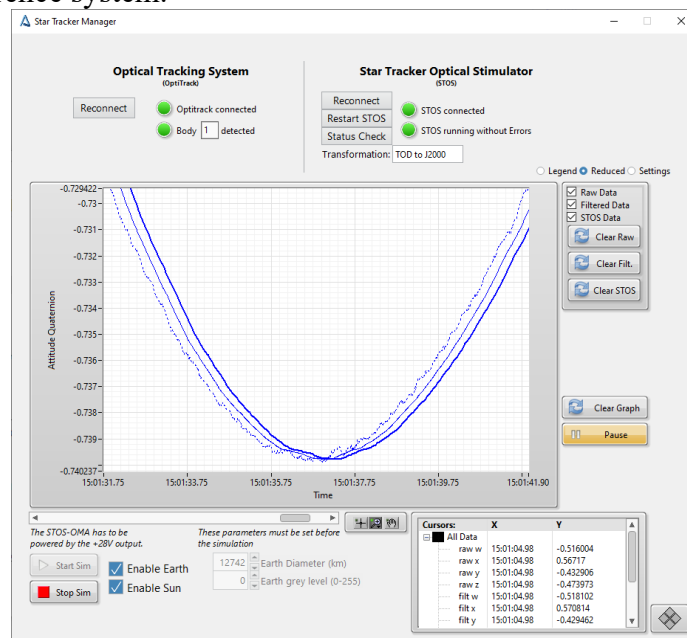


Figure 13 Interface of the ST-Manager showing delays (about 550ms) to one quaternion. Dotted Line: Raw data from motive; Thin line: Sliding average; Bold line: Feedback from STOS.

## 5 NANO SATELLITE PLATFORM

Downscaling the test bed to accommodate Nano satellites has been a recurring request. The main issue is to reduce air bearing size, platform MOI and disturbance torques to Nano satellite level. Also, the testing principle is different. Nano satellites are often tested with the complete satellite on the air bearing, rather than only the attitude control system. This could be due to the model approach (usually Proto-Flight-Model (PFM), without an ACS EM) combined with shorter integration and testing times. There is usually not time and/or money to set-up a specific ACS EM for a Nano satellite mission. Therefore, the Nano satellite platform was designed

- without power supply to DUT, since the satellite comes with its own
- with as low a MOI as possible, since any platform MOI adds to the DUT MOI → no platform electronics or power supply
- with manual CoG calibration, since the lack of power and electronics make a wireless calibration impossible

The air bearing itself is also much smaller, requiring a smaller mechanical interface and providing lower disturbance torques but also much less loading capability.

Though the performance and size of Nano satellites is increasing, the first design was for testing CubeSats up to 3U. The torque capabilities of these CubeSats are often below  $10^{-5}$  Nm, therefore the disturbance torques from the bearing should be well below that, at least for the main rotation axis (z-axis). The NanoSat Add-on (so named, because it can be added to the small satellite table configuration, utilizing the environmental simulation from the larger test bed) achieved a performance of  $<1.5 \cdot 10^{-6}$  Nm disturbance torque around z-axis, and  $<6.5 \cdot 10^{-5}$  Nm around x/y. The friction in the bearing was measured to be below  $3 \cdot 10^{-7}$  Nm. This is almost a magnitude smaller than what we see in the larger bearing (compare to section 4.1) and therefore a great result.

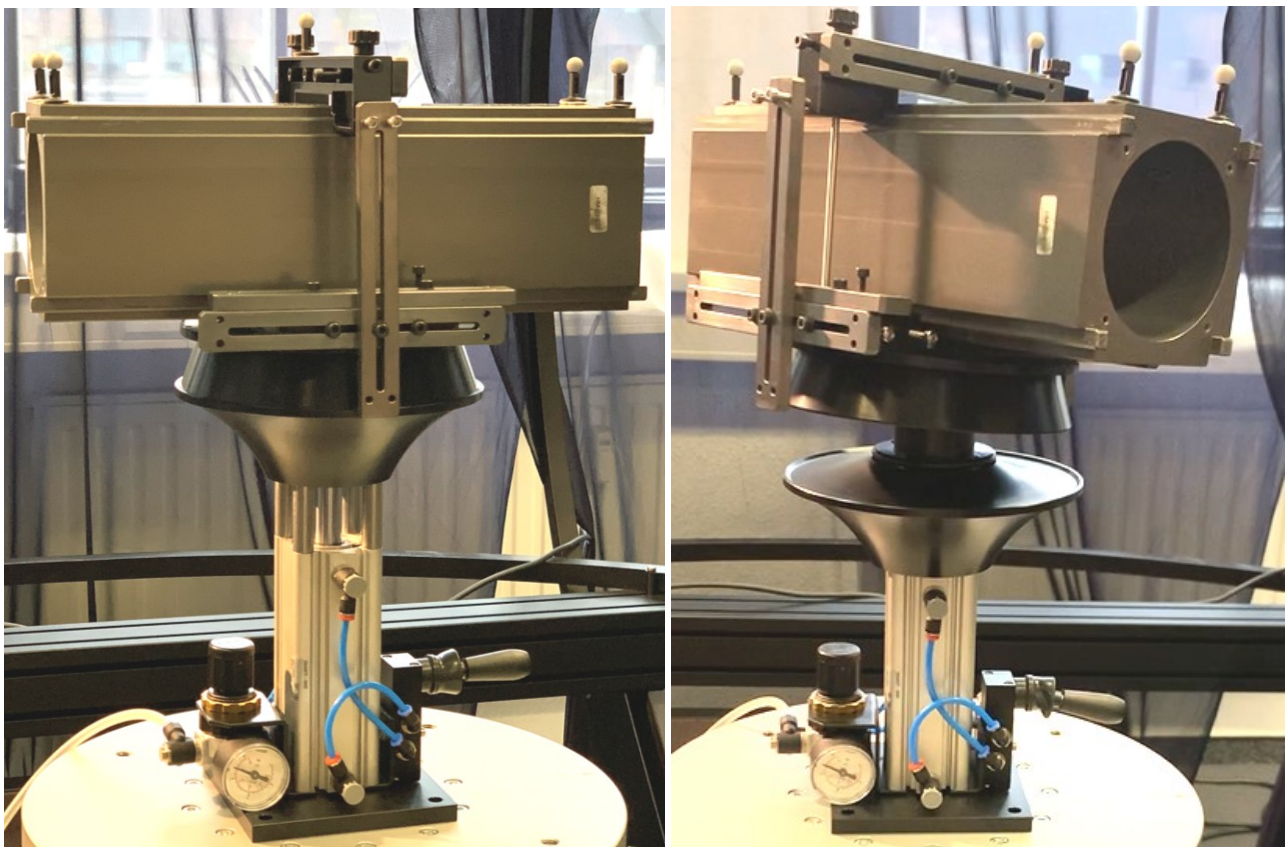


Figure 14 NanoSat Add-on with 3U CubeSat satellite dummy; extended support (left) and free floating (right)

Since the bearing is sensitive, collisions should be avoided. Much like the larger bearing, the design has an integration support, which can be raised and lowered pneumatically (see Figure 14). In the raised position, the DUT and platform are lifted off the air bearing. Now, assembly or disassembly of the DUT can take place without endangering the performance of the air bearing.

As mentioned above, the calibration is performed manually to keep the MOI of the set-up to a minimum. Next to precise positioning of the DUT in the centre, sliders can be added and easily moved to roughly calibrate the CoG. For fine tuning, M4 screws can be placed in multiple locations, each single rotation moving the screw mass (2.345 g) over 0.7 mm, achieving a torque of  $8.05 \cdot 10^{-6}$  Nm.

## 6 SUMMARY, CONCLUSION AND OUTLOOK

In past small satellite missions, an ACS test bed has been a critical tool for developing and testing ACS algorithms, verifying ACS performance, testing flight operation procedures and FDIR mechanisms and verifying software updates throughout the satellite's lifetime. Issues that could have become critical in orbit were detected and corrected during ACS verification. Test cases ranged from simple sign tests to a sequence of attitude manoeuvres for autonomous formation flight.

The state-of-the-art test bed allows small satellite testing with disturbances similar to what is expected in orbit. Multiple ACS sensors can be stimulated, namely sun sensors, magnetic field sensors, GNSS receivers and star trackers. The integration of a star simulation dynamically coupled to the platform attitude, is the latest addition to the testbed. Moreover, an autocalibration of the CoG has been developed that relies solely on geometric parameters of the system and requires no MOI estimation. The NanoSat Add-on extends the test bed capabilities to Nano satellites and future developments focus on extending it, to include testing capabilities for 12U and 24U satellites as well as reducing the disturbance torques even more.

## 7 REFERENCES

- [1] Terzibaschian, T., *BIRD attitude determination and control system*, Small Satellites for Earth Observation, Digest of the 3rd International Symposium of the International Academy of Astronautics, Berlin, April 2-6, 2001, 3, page 405. Wissenschaft & Technik Verlag. 3rd IAA Symposium on Small Satellites for Earth Observation, April 2-6, 2001, Berlin, Germany. ISBN 3-89685-566-2
- [2] Nicolai A., et al. *Software and hardware in the loop tests - from pico to small satellites with air bearing test stands*, IAC-22,B4,6A,x73058, 73<sup>rd</sup> International Astronautical Congress (IAC), Paris, France, 18-22 September 2022.
- [3] <https://www.optitrack.com/>, last visited 17.05.2023
- [4] T. Shima et al. *Automatic balancing for a three-axis spacecraft simulator*, Transactions of the Japan Society for Aeronautical and Space Sciences, Aerospace Technology Japan., vol. 8, no. 27, pp. 15–22, 2010.
- [5] J. J. Kim and B. N. Agrawal, *Automatic mass balancing of air-bearing-based three-axis rotational spacecraft simulator*, Journal of Guidance, Control, and Dynamics, vol. 32, no. 3, pp. 1005–1017, 2009.